Available online at www.sciencedirect.com
ScienceDirect
Powder Technology 176 (2007) 66 – 71
POWDER TECHNOLOGY
www.elsevier.com/locate/powtec

Effect of bi- and trimodal size distribution on the superficial hardness of Al/SiC$_p$ composites prepared by pressureless infiltration

M. Montoya-Dávila [a], M.A. Pech-Canul [b], M.I. Pech-Canul [a,*]

[a] Cinvestav Saltillo. Carr. Saltillo-Mty. Km 13, Saltillo Coah. México, 25900, Mexico
[b] Cinvestav Mérida. Km. 6 Antigua carretera a Progreso Apdo. Postal 73, Cordemex, 97310, Mérida, Yuc, Mexico

Received 29 March 2006; received in revised form 12 September 2006; accepted 15 February 2007
Available online 23 February 2007

Abstract

The effect of particle size distribution on the superficial hardness of Al/SiC$_p$ composites prepared by pressureless infiltration, as well as on the microhardness and fracture toughness (K_{IC}) of particulate silicon carbide (SiC$_p$) was investigated. Preforms with 0.6 volume fraction of SiC powders (10, 68 and 140 μm) with monomodal, bimodal and trimodal distribution were infiltrated with the alloy Al–15.52 Mg–13.62 Si (wt.%) in argon followed by nitrogen at 1100 °C for 60 min. Results show that density behaves linearly with increase in particle-size-distribution whilst superficial hardness, microhardness and fracture toughness exhibit all a parabolic behavior. Superficial hardness behavior can be explained by the combined effect of work-hardening in the alloy matrix and particle-to-particle impingement. Due to the highly covalent nature of SiC, the parabolic response shown by microhardness and K_{IC} cannot be attributed to a dislocation mechanism as in strain-hardening.

Keywords: SiC powders; Particle size distribution; Metal matrix composites (MMCs); Liquid metal infiltration; Fracture toughness; Hardness; Work-hardening

1. Introduction

Infiltration of porous ceramic preforms by liquid metals is probably the most convenient route to fabricate metal matrix composites (MMCs) with high volume fraction of the ceramic reinforcement. It allows obtaining near- or net-shape composites with uniform distribution of the reinforcements and high dimensional stability. Most of the research efforts on Al/SiC composites with high volume fraction of SiC have been directed toward applications demanding low density, elevated thermal conductivity, low coefficient of thermal expansion and high modulus [1–9]. Electronic packaging materials with thermal conductivity and thermal expansion coefficient similar to those of ordinary elements in microelectronic systems are typical examples of this type of MMCs [1–5]. To increase the volume fraction of the ceramic phase it is necessary to accommodate reinforcements of substantially different sizes into the porous ceramic preforms. Consequently, depending on the application and desired properties, particle-size-distribution becomes a key parameter in process development and optimization. Certainly, processing parameters and the resulting properties in the composites will also depend on the infiltration mode, that is, without assistance or by the application of pressure (or vacuum). Most of the work done on composites with high volume fraction of the ceramic phase has centered on the pressure assisted infiltration technique aimed at preparing materials with bimodal distribution of reinforcements [5–8]. Investigations involving more than two particle sizes are rather limited. For instance, Chen and co-workers conducted a comprehensive investigation on four-modal distribution and volume fraction of SiC powders as high as 0.74 using the squeeze casting technique under pressures between 25 and 200 MPa [6].

Development of non-assisted or pressureless infiltration routes not only has an impact on processing costs but also helps in resolving many technical issues. In contrast with the pressure assisted infiltration technique, the non-assisted infiltration route considerably minimizes the risk of ceramic preform deformation or even worse its rupture during processing. Investigations related to the use of pressureless infiltration for the preparation of Al/SiC$_p$ composites with high volume fraction of the reinforcements (between 0.40 and 0.70) are also scarce [9]. To our knowledge,

* Corresponding author. Tel.: +52 844 438 9600x9678; fax: +52 438 9610.
E-mail address: martin.pech@cinvestav.edu.mx (M.I. Pech-Canul).

0032-5910/$ - see front matter
doi:10.1016/j.powtec.2007.02.008

until now there are no reports connected with the use of the capillary effect for the infiltration of ceramic preforms with trimodal distribution or higher. Cui used the pressureless melt infiltration route to examine the potential of Al/SiC$_p$ composites with high volume fraction of the ceramic for use as optomechanical components for space-based optical systems and electronic packages for avionics systems [9]. The author reported some composite properties including the coefficient of thermal expansion, thermal conductivity, flexural strength and Young's modulus. However, no discussion about the effect of particle size and particle size distribution on the composite properties was presented. Furthermore, the size or sizes of the SiC powders used in the investigation were not specified [9].

It is expected that MMCs with high volume fraction and multimodal size distribution of the ceramic reinforcements will exhibit physical and mechanical properties significantly different from those of composites with low volume fraction of the ceramic phase. The related literature shows that most of the effort has focused on studying the deformation behavior of the composites and that little or no attention has been paid to the reinforcements themselves [10–20]. The objective of this work was to investigate the effect of bimodal and trimodal distribution of particulate reinforcements on the superficial hardness of Al/SiC composites processed via pressureless infiltration as well as on the microhardness and fracture toughness of SiC$_p$. This work is centered on the potential to produce Al/SiC$_p$ composites with high volume fraction of the ceramic by the pressureless infiltration method using up to three different particle sizes.

2. Experimental procedures

Ceramic preforms with 0.6 volume fraction of α-SiC powders were prepared using three different particles sizes (10, 68 and 140 μm), three particle size distributions (monomodal, bimodal and trimodal) and different particle size ratios (1:1, 3:1, 1:3, 2:2:2, 3:2:1, 3:1:2). Particle-size-ratio designation involves both, the type of preform (bimodal or trimodal) and the proportion of each particle size. As for the latter aspect, systematically bimodal and trimodal preforms consist of *small/large* and *small/medium/large* particles, respectively. For instance, 3:1 represents a bimodal preform prepared with three parts of small SiC particles and one part of large ones; 3:1:2 stands for a trimodal preform made up of three parts of small particles, one part of medium and two parts of large ones. Monomodal preforms are just designated with the corresponding particle size. To prevent SiC attack by the liquid aluminum alloy, the SiC particles were mixed with 10 wt.% of SiO_2 powders (~346 μm). Incorporation of at least 6 wt.% SiO_{2p} has been proven to be effective in preventing formation of the unwanted Al_4C_3 phase [21]. Then the powders were mixed with 8 wt.% dextrin as binder, placed into a steel mould and compacted uniaxially using a hydraulic press (~3.5 MPa) to produce plate-shaped preforms of 3 cm × 4 cm × 0.5 cm. The dextrin was partially eliminated from the preforms heating in an air furnace for 2 h at 125 °C and then for two more hours at 225 °C. The organic binder is completely eliminated during the heating event in the infiltration trials. An aluminum alloy (Al–15.52 Mg–13.62 Si) suitable for pressureless infiltration was specifically fabricated for this investigation in an induction furnace. Essentially under the processing conditions the aluminum alloy wets the SiC particles. The alloy chemical composition is shown in Table 1.

Infiltration trials were performed in a horizontal tube furnace with a 6.5 cm diameter alumina tube closed at both ends with end-cap fittings to control the process atmosphere. The preform and approximately 32 g of the alloy were placed in a ceramic container and the whole assembly was positioned in the center of the tube. The system was heated at a rate of 15 °C/min up to 1100 °C, held at that temperature for 60 min and then cooled down with same rate to room temperature. During the heating period and up to 1000 °C, the specimens were treated in ultra high purity (UHP) argon. Then, in order to enhance the wetting of the preform by the liquid alloy, a change in the atmosphere from Ar to UHP N_2 was conducted at 1000 °C [22]. Once the system was cooled down to room temperature, composite specimens were prepared for density determination (using the Archimedes' principle), microstructure characterization and mechanical property evaluation. Accordingly, the composites were characterized by X-ray diffraction (XRD), scanning electron microscopy (SEM) and energy dispersive X-ray spectroscopy (EDX). In order to determine the average distance between particles, preforms with monomodal, bimodal and trimodal size distribution were mounted in phenolic resin and polished using standard procedures. The distance between particles in the preforms was measured using an optical microscope (OM) equipped with an image analyzer (Image Pro-Plus 4).

Rockwell hardness tests were carried out using a steel ball (1/16 in diameter), according to the ASTM E-18 standard procedures. Vickers microhardness tests were performed on medium and large SiC particles, using loads of 200, 250 and 300 g in accordance with ASTM E384-84 standard procedures. The fracture toughness of SiC$_p$ was evaluated from the crack extensions produced during the microindentations according to [23]:

$$K_{\mathrm{IC}} = \frac{\zeta (E/H)^{\frac{1}{2}} P}{c^{\frac{3}{2}}} \tag{1}$$

where E is the modulus of elasticity in GPa, P is the load in kg, H is the microhardness in GPa, c is the crack length in meters, and ζ is a constant parameter (for ceramics is 0.016 ± 0.004) [2].

3. Results and discussion

3.1. Microstructure characterization

Results from X-ray diffraction revealed that $MgAl_2O_4$, AlN, MgO and Mg_2Si were formed in situ during processing. These

Table 1
Chemical composition of the alloy prepared for pressureless infiltration (wt.%)

Mg	Si	Fe	Mn	Zn	Others	Al
15.52	13.62	0.99	0.15	0.13	2.61	Balance

phases were identified in the composites in addition to Al, Si and SiC. Fig. 1(a), (b), and (c) are typical diffractograms corresponding to composites with monomodal, bimodal and trimodal size distribution, respectively. As expected, incorporation of SiO_2 particles successfully helped to avoid Al_4C_3 formation in the composites. The reaction mechanisms for formation of $MgAl_2O_4$, AlN, MgO and Mg_2Si in Al/SiC composites involving Al–Mg, Al–Si alloys and SiO_2 have been extensively discussed by others [24–28]. Therefore, they will not be detailed in this work. Fig. 2(a), (b), and (c) show typical microstructures in composites with monomodal, bimodal, and trimodal distribution, respectively.

3.2. Physical and mechanical property evaluation

Results show that the measured densities in the composites (2.77–2.91 g/cm^3) are similar to those reported for Al/SiC composites prepared by the squeeze casting technique [6]. As shown in Fig. 3, density increases linearly with particle-size-distribution. On the other hand it was observed that particle-size-ratio has no significant effect on the composites density. Also it should be noted that residual porosity varied between 1% and 4%, and that there is no correlation between this response variable neither with particle-size-distribution nor with particle-size-ratio.

Results from Rockwell hardness tests show that superficial hardness exhibits a parabolic behavior with increase in particle size distribution (see Fig. 4). The average hardness values of composites with monomodal, bimodal and trimodal distribution are 39±3.1, 63±2.9 y 66±0.6 HR30T respectively. Each of these values represents the average superficial hardness of all specimens with the same particle size distribution regardless of particle size ratio. The observed parabolic behavior can be explained in terms of the deformation undergone by the metallic matrix and to the concomitant particle–particle interference during the spherical indentation. Image analysis in the preforms before infiltration showed that the distance between particles varies significantly on going from monomodal to bi- and trimodal size distribution. Explicitly, for a monomodal preform with particle size of 68 μm, the distance between particles is 23 μm while for bimodal and trimodal distribution the average distances are 7.00 and 7.8 μm,

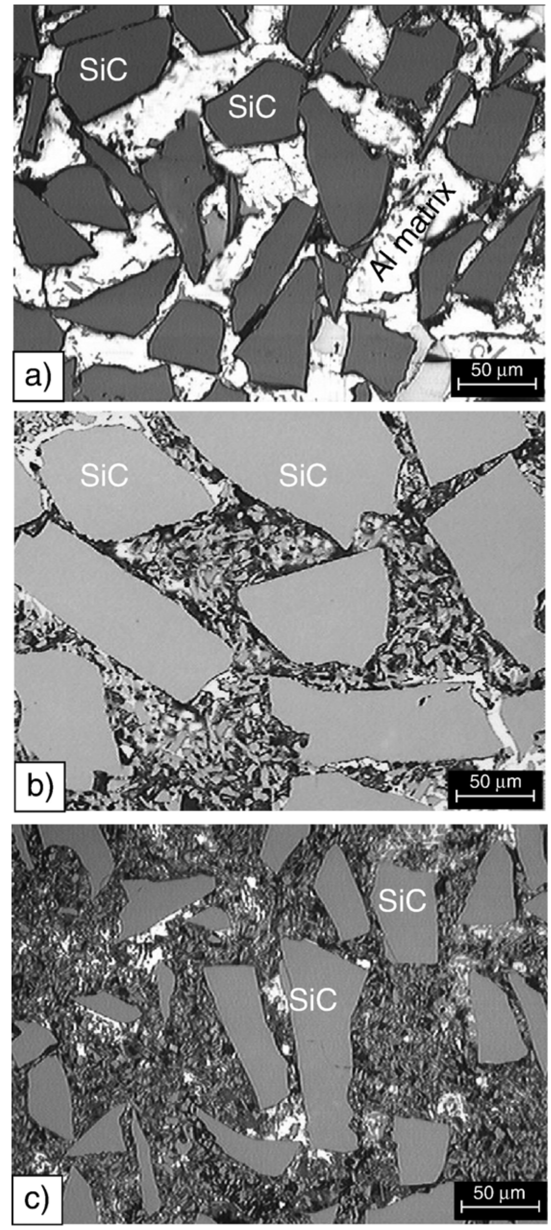

Fig. 2. Optical photomicrographs showing the typical microstructure in composite with a) monomodal, b) bimodal and c) trimodal distribution of SiC particles.

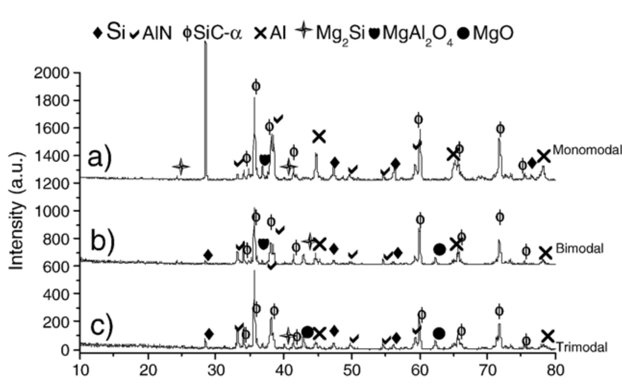

Fig. 1. Typical X-ray diffraction patterns in composites with monomodal, bimodal and trimodal size distribution.

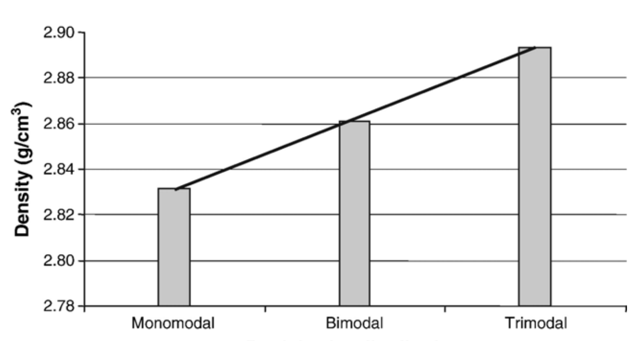

Fig. 3. Effect of SiC particle size distribution on the composites densities.

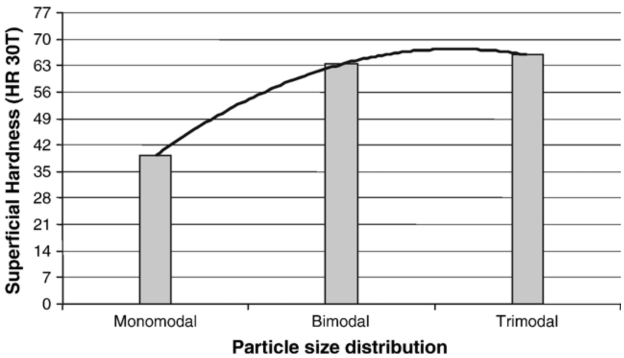

Fig. 4. Effect of SiC particle size distribution on the composites superficial hardness.

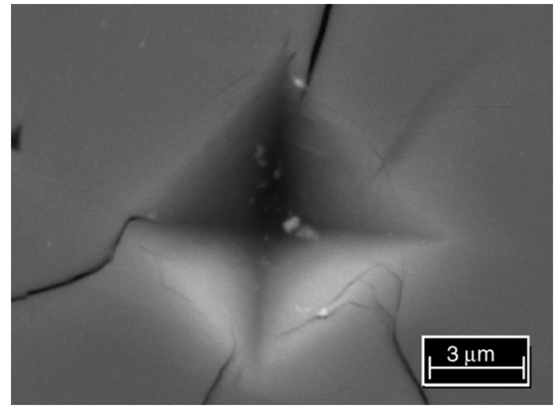

Fig. 6. Photomicrograph of a tested SiC particle of 68 μm, showing a well-defined permanent deformation.

respectively. Thus, during spherical indentation and under the same applied load, particles in composites with tri- and bimodal distribution will collide more rapidly than those in composites with monomodal distribution, leading to a more extensive plastic deformation in the metallic matrix of monomodal specimens. Therefore, the higher the particle size distribution the higher the blockage between the SiC particles and the higher the magnitude of the stresses developed at the metal/reinforcement interface. In other words, greater stresses will be required to produce further plastic deformation on going from monomodal to bimodal and trimodal distribution. Essentially this behavior can be associated to a dislocation mechanism in the metallic phase known as work-hardening or strain-hardening.

The incidence of work-hardening in particulate metal matrix composites was studied previously by Corbin and Wilkinson establishing a model to predict the flow of a particulate-reinforced alloy [19]. Beyond the elastic limit the model predicts an increase in the initial work-hardening rate with increasing particle content. Nan and Clarke proposed that depending on the particle size range a different model might be applicable [29]. Modeling the deformation response of MMCs in terms of an effective medium approach combined with the essential features of dislocation plasticity, Nan and Clarke found a good correlation with experimental stress–strain curves [29]. In the current work particle volume fraction was constant (0.6); therefore, work-hardening in the metallic matrix can only be attributed to the combined effect of particle size distribution and particle impingement.

The SiC Vickers-hardness values in composites with monomodal, bimodal and trimodal size distribution are 2339±223, 3360±320 and 3464±368 kg/mm^2, respectively. And as shown in Fig. 5, SiC$_p$ microhardness exhibits a parabolic behavior with increment in particle size distribution. Fig. 6 is the photomicrograph of a tested SiC particle of 68 μm, showing a well-defined permanent deformation produced by the indentation and the propagation of some cracks. Interestingly and similar to the microhardness behavior the magnitude of fracture toughness (K_{IC}) also increases parabolically with increase in particle size distribution (see Fig. 7). Like in the case of density, Vickers microhardness and K_{IC} values in the graphs represent the average from all composites having the same particle size distribution (monomodal, bimodal or trimodal), irrespective of particle size ratio.

Most single-crystal and polycrystalline ceramics fracture in a brittle mode with no plastic deformation. This behavior is determined by a competition between creation/movement of dislocations and stress concentration at microstructural defects. If the applied stress first reaches the yield stress for dislocation motion, plastic deformation will occur. If the local stress first reaches the critical fracture stress at a microstructural defect (such as a pore, crack or inclusion) in the material, brittle fracture will occur. For plastic deformation to be possible in ceramic materials, it has been determined that five independent slip systems must be present in the crystal structure [30]. Most ceramics have three or less slip systems at room temperature

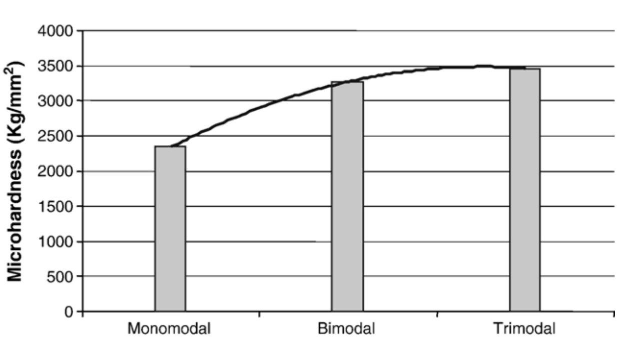

Fig. 5. SiC$_p$ microhardness as a function of particle size distribution.

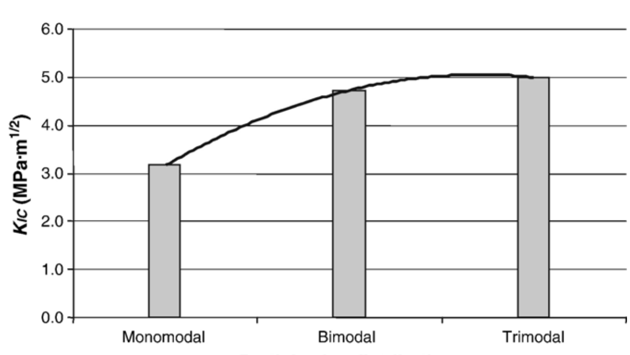

Fig. 7. SiC$_p$ fracture toughness (K_{IC}) as a function of particle size distribution.

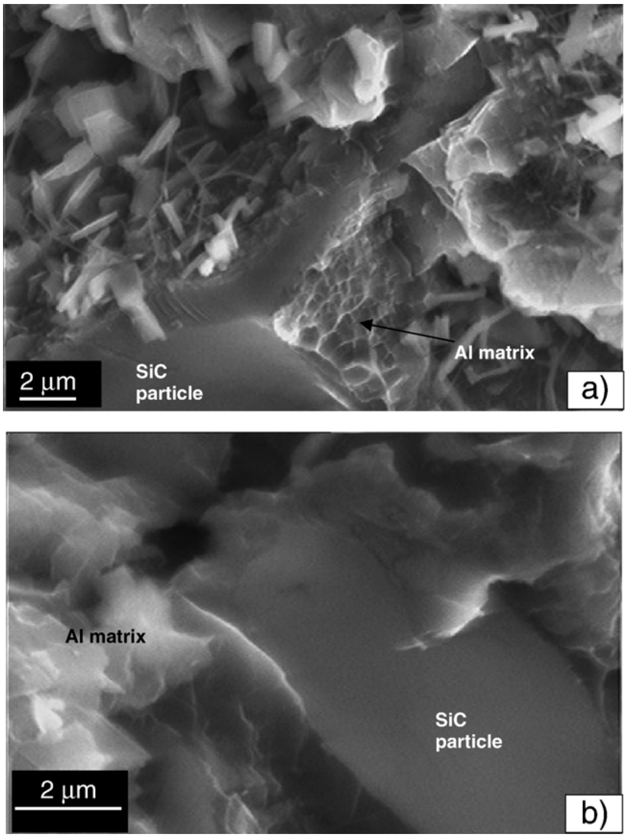

Fig. 8. SEM photomicrographs of typical fracture surfaces in the Al/SiC$_p$ composites, showing the good bonding that exists between the SiC particles and the aluminum matrix.

and only a few have five at elevated temperature. Therefore under an applied load, plastic or permanent deformation is likely to occur but locally or in an extremely limited degree. Accordingly, the parabolic behavior exhibited by microhardness and K_{IC} cannot be directly associated to a work-hardening effect in SiC. A hypothetical explanation for this behavior would be load transfer from the indented particle to the metallic matrix and then to other neighboring SiC particles through the ceramic/metal interfaces. This would require extensive dislocation mobility, which for a highly covalent material like SiC it is rather difficult to occur. Certainly, the triaxial compression state of stresses developed during the indentation leads to enough dislocation mobility to produce the indent. Primarily this is because the alpha polymorph of SiC has many polytypes corresponding to different packing sequences of parallel layers of tetrahedra [31]. However, outside the small or tiny region resulting from the indentation there is no mobility. In this sense, more detailed studies would be required to explain the parabolic behavior observed in SiC$_p$ Vickers-hardness and fracture-toughness with increment in particle size distribution.

In general, K_{IC} values are slightly higher than those reported previously for Al/SiC$_p$ composites processed by pressureless infiltration with monomodal distribution, using SiC particles of 75 μm (3.7±0.5 MPa m$^{1/2}$) [32]. Although the particle sizes used in this work are different from those employed previously in monomodal composites [32], the current results confirm the superior fracture toughness of SiC particles in composites with bi- and trimodal distributions.

Although a discussion on the composites modulus-of-rupture (MOR) is beyond the scope of this paper, here we briefly present some results on the fracture surface analysis carried out in specimens after four-point bending tests. Fig. 8(a) and (b) are SEM photomicrographs of typical fracture surfaces in the composites. In spite of the extensive plastic deformation and ductile fracture undergone by the metallic phase, the good condition of the reinforcement/matrix interface (see Fig. 8(b)) after the flexural trials suggests that the bonding between the SiC particles and the metallic matrix is strong enough to support the load transfer from the matrix to the reinforcements. These interface bonding characteristics are worthy of mentioning, particularly for composites processed without the assistance of pressure or vacuum.

4. Summary and conclusions

The microhardness and fracture toughness of SiC$_p$ as well as the superficial hardness of Al/SiC$_p$ composites with mono-, bi- and trimodal distribution of reinforcements prepared by non-assisted infiltration were evaluated. Microhardness tests revealed that after processing the SiC particles are in good condition, exhibiting K_{IC} values similar to those reported in the literature for polycrystalline SiC [30]. Results show that while density increases linearly with particle size distribution, the composites superficial hardness as well as microhardness/fracture toughness of SiC$_p$ show all a parabolic behavior. In the case of superficial hardness this behavior is attributed to a work-hardening effect in the metallic matrix and to particle–particle impingement. However, from our current results and due to the highly covalent nature of SiC, the parabolic behavior observed in microhardness and fracture toughness cannot be directly explained by the same dislocation model.

Acknowledgements

Authors gratefully acknowledge Semarnat-Conacyt for financial support under contract # 2002-C01-1302. Mr. Montoya-Dávila is very thankful to Conacyt for providing a scholarship. Authors also express gratitude to Prof. R.N. Katz for his valuable comments about the work. Also thanks to Microabrasivos de México for providing the SiC powders and Mr. Felipe Márquez Torres for assistance during the microscopic analysis.

References

[1] W.H. Hunt Jr., M.K. Premkumar, Novel materials for electronic packaging and thermal management, JOM (July 1992) 8–10.
[2] A.H. Kumar, R.R. Tummala, The past, present and future of multilayer ceramic multichip in electronic packaging, JOM (July 1992) 10–14.
[3] C. Zweben, Metal-matrix composites for electronic packaging, JOM (July 1992) 15–23.
[4] M.K. Premkumar, W.H. Hunt Jr., R.R. Sawtell, Aluminum composite materials for multichip modules, JOM (July 1992) 24–27.
[5] H.S. Lee, C.S. Lee, J.R. Lee, Pressure infiltration casting process and thermal properties of high volume fraction SiC$_p$/Al composites for electronic packaging, Aluminum Transactions 3 (2000) 1–6.

[6] C.Y. Chen, C.G. Chao, Effect of particle-size distribution on the proprieties of high volume-fraction SiC_P-Al-based composites, Metall. Mater. Trans., A Phys. Metall. Mater. Sci. 31A (2000) 2351–2359.

[7] J.M. Molina, R.A. Saravanan, R. Arpón, C. García-Cordovilla, E. Louis, J. Narciso, Pressure infiltration of liquid aluminum into packed SiC particulate with bimodal size distribution, Acta Mater. 50 (2002) 247–257.

[8] R. Arpón, J.M. Molina, R.A. Saravanan, C. García-Cordovilla, E. Louis, J. Narciso, Thermal expansion behaviour of aluminum/SiC composites with bimodal particle distributions, Acta Mater. 51 (2003) 3145–3156.

[9] Y. Cui, High volume fraction SiC_p/Al composites prepared by pressureless melt infiltration: processing, properties and applications, Key Eng. Mater. 249 (2003) 45–48.

[10] M. Manoharan, J.J. Lewandowski, In-situ deformation studies of an aluminum metal-matrix composite in an scanning electron microscope, Scr. Metall. 23 (1989) 1801–1804.

[11] S. Kumai, J.E. King, J.F. Knott, Fatigue in SiC-particulate-reinforced aluminum alloy composites, Mater. Sci. Eng., A Struct. Mater.: Prop. Microstruct. Process. 146 (1991) 317–326.

[12] Y. Li, F.A. Mohamed, An investigation of creep behavior in an SiC–2124 Al composite, Acta Mater. 45 (11) (1997) 4775–4785.

[13] T.W. Gustafson, P.C. Panda, G. Song, R. Raj, Influence of microstructural scale on plastic flow behavior of metal matrix composites, Acta Mater. 45 (4) (1997) 1633–1643.

[14] S. Shan, H. Nayeb-Hashemi, Fatigue-life prediction of SiC particulate reinforced aluminum alloy 6061 matrix composite using AE stress delay concept, J. Mater. Sci. 34 (1999) 3263–3273.

[15] M. Singh, D.P. Mondal, R. Dasgupta, A.K. Jha, Combined effect of load, abrasive size and sliding distance on the high stress abrasive wear behavior of an aluminum composite, Alum. Trans. 3 (1) (2000) 7–15.

[16] N. Nagendra, V. Jayaram, Fracture and R-curves in high volume fraction Al_2O_3 composites, J. Mater. Res. 15 (5) (2000) 1131–1144.

[17] N. Nagendra, V. Jayaram, Influence of matrix characteristics on fracture toughness of high volume fraction Al_2O_3/Al–AlN composites, J. Mater. Res. 15 (5) (2000) 1145–1153.

[18] A. Forn, M.T. Baile, E. Rupérez, Spinel effect on the mechanical properties of metal matrix composite AA6061/$(Al_2O_3)_p$, J. Mater. Process. Technol. 143–144 (2003) 58–61.

[19] S.F. Corbin, D.S. Wilkinson, The influence of particle distribution on the mechanical response of a particulate metal matrix composite, Acta Metall. Mater. 42 (4) (1994) 1311–1318.

[20] M.T. Kiser, F.W. Zok, D.S. Wilkinson, Plastic flow and fracture of a particulate metal matrix composite, Acta Mater. 44 (9) (1996) 3465–3476.

[21] M. Rodríguez-Reyes, M.I. Pech-Canul, J.C. Rendón-Angeles, J. López-Cuevas, Limiting the development of Al_4C_3 to prevent degradation of Al/SiC_p composites processed by pressureless infiltration, Compos. Sci. Technol. 66 (2006) 1056–1062.

[22] M.I. Pech-Canul, R.N. Katz, M.M. Makhlouf, Optimum parameters for wetting silicon carbide by aluminum alloys, Metall. Mater. Trans., A Phys. Metall. Mater. Sci. 31A (2000) 565–573.

[23] G.R. Antis, P. Chantikul, B.R. Lawn, D.B. Marshall, A critical evaluation of indentation techniques for measuring fracture toughness: I. Direct crack measurements, J. Am. Ceram. Soc. 64 (9) (1981) 533–538.

[24] L. Salvo, G.L. 'Espérance, M. Suéry, J.G. Legoux, Interfacial reactions and age hardening in Al–Mg–Si metal matrix composites with SiC particles, Mater. Sci. Eng., A Struct. Mater.: Prop. Microstruct. Process. A177 (1994) 173–183.

[25] Q. Hou, R. Mutharasan, M. Kockzak, Feasibility of aluminum nitride formation in aluminum alloys, Mater. Sci. Eng., A Struct. Mater.: Prop. Microstruct. Process. 195 (1995) 121–129.

[26] Z. Shi, J.M. Yang, J.C. Lee, D. Zhang, H.I. Lee, R. Wu, The interfacial characterization of oxidized $SiC_{(p)}$/2014 Al composites, Mater. Sci. Eng., A Struct. Mater.: Prop. Microstruct. Process. A303 (2001) 46–53.

[27] Z. Shi, S. Ochiai, M. Hojo, J. Lee, M. Gu, H. Lee, Joining characteristics of oxidized SiC particles reinforced Al–Mg matrix composite prepared by reaction infiltration processing, J. Mater. Res. 16 (2) (2001) 400–406.

[28] A. Ureña, E.E. Martínez, P. Rodrigo, L. Gil, Oxidation treatments for SiC particles used as reinforcement in aluminum matrix composites, Compos. Sci. Technol. 64 (2004) 1843–1854.

[29] C.-W. Nan, D.R. Clarke, The influence of particle size and particle fracture on the elastic/plastic deformation of metal matrix composites, Acta Mater. 44 (9) (1996) 3801–3811.

[30] D.W. Richerson, Modern Ceramic Engineering, Marcel Dekker Inc., New York, 1992.

[31] B. Wachtman, Mechanical Properties of Ceramics, J. Wiley & Sons Inc., New York, 1996.

[32] Parras-Medécigo E.E. Processing and characterization of functionally graded Al/SiC_p composites by non-assisted infiltration, MSc Thesis, Cinvestav Saltillo. Saltillo Coah. México, 2001.